# Coincident Activation of Glutamate Receptors Enhances GABA$_A$ Receptor-Induced Ionic Plasticity of the Intracellular Cl$^-$-Concentration in Dissociated Neuronal Cultures

Lisa Halbhuber , Cécilia Achtner , Heiko J. Luhmann , Anne Sinning and Werner Kilb *

Institute of Physiology, University Medical Center Mainz, Johannes Gutenberg University, Mainz, Germany

Massive activation of γ-amino butyric acid A (GABA$_A$) receptors during pathophysiological activity induces an increase in the intracellular Cl$^-$-concentration ([Cl$^-$]$_i$), which is sufficient to render GABAergic responses excitatory. However, to what extent physiological levels of GABAergic activity can influence [Cl$^-$]$_i$ is not known. Aim of the present study is to reveal whether moderate activation of GABA$_A$ receptors mediates functionally relevant [Cl$^-$]$_i$ changes and whether these changes can be augmented by coincident glutamatergic activity. To address these questions, we used whole-cell patch-clamp recordings from cultured cortical neurons [at days *in vitro* (DIV) 6–22] to determine changes in the GABA reversal potential (E$_{GABA}$) induced by short bursts of GABAergic and/or synchronized glutamatergic stimulation. These experiments revealed that pressure-application of 10 short muscimol pulses at 10 Hz induced voltage-dependent [Cl$^-$]$_i$ changes. Under current-clamp conditions this muscimol burst induced a [Cl$^-$]$_i$ increase of 3.1 ± 0.4 mM (*n* = 27), which was significantly enhanced to 4.6 ± 0.5 mM (*n* = 27) when glutamate was applied synchronously with the muscimol pulses. The muscimol-induced [Cl$^-$]$_i$ increase significantly attenuated the inhibitory effect of GABA, as determined by the GABAergic rheobase shift. The synchronous coapplication of glutamate pulses had no additional effect on the attenuation of GABAergic inhibition, despite the larger [Cl$^-$]$_i$ transients under these conditions. In summary, these results indicate that moderate GABAergic activity can induce functionally relevant [Cl$^-$]$_i$ transients, which were enhanced by coincident glutamate pulses. This ionic plasticity of [Cl$^-$]$_i$ may contribute to short-term plasticity of the GABAergic system.

Keywords: Cl$^-$-homeostasis, KCC2, reversal potential, rheobase, ionic plasticity, GABA(A) receptors, dissociated cell culture, mouse

## INTRODUCTION

γ-amino butyric acid (GABA), the main inhibitory neurotransmitter in the adult mammalian brain, acts *via* ionotropic GABA$_A$ and metabotropic GABA$_B$ receptors (Mody and Pearce, 2004; Farrant and Kaila, 2007). GABA receptors not only control the excitability in the brain, but are essential for specific neuronal processes, like regulating size of neuronal assemblies, gating propagation of

activity, mediating neuronal plasticity, and controlling oscillatory activity (Whittington and Traub, 2003; Fagiolini et al., 2004; Jonas et al., 2004; Mody and Pearce, 2004; Pouille and Scanziani, 2004). As ligand-gated chloride channels, GABA$_A$ receptors permit in the adult nervous system Cl$^-$ influx, which hyperpolarizes the membrane and mediates an inhibitory action. In addition, the opening of GABA$_A$ receptors induces shunting inhibition due to a decreased membrane resistance (Farrant and Kaila, 2007). The Cl$^-$ influx, and thus the inhibitory hyperpolarization of the membrane potential, depends on a negative equilibrium potential for Cl$^-$ (E$_{Cl}$), which is determined by a low intracellular chloride concentration ([Cl$^-$]$_i$). This low [Cl$^-$]$_i$ is maintained by the chloride extruder potassium chloride cotransporter 2 (KCC2) in the adult mammalian brain (Rivera et al., 1999, 2005; Blaesse et al., 2006, 2009). In accordance with the central role of KCC2 for the function of the GABAergic systems, dysfunctions of Cl$^-$ extrusion has been linked to neurological diseases, like epilepsy or chronic pain (Kahle et al., 2008; Kaila et al., 2014a; Silayeva et al., 2015). Thus, KCC2 has been identified as a putative target for anticonvulsive therapies (Löscher et al., 2013; Puskarjov et al., 2014a; Moore et al., 2018) and pain control (Gagnon et al., 2013; Kahle et al., 2014a; Lavertu et al., 2014).

As GABA$_A$ receptors mediate a considerable Cl$^-$ conductance, they directly affect [Cl$^-$]$_i$, a process that is termed "ionic plasticity" (Rivera et al., 2005; Jedlicka and Backus, 2006; Wright et al., 2011; Raimondo et al., 2012b; Kaila et al., 2014a). It has been shown that massive GABAergic activity induces considerable and functionally relevant changes in [Cl$^-$]$_i$ (Ballanyi and Grafe, 1985; Thompson and Gähwiler, 1989; Kuner and Augustine, 2000; Fujiwara-Tsukamoto et al., 2003; Isomura et al., 2003; Raimondo et al., 2015; Moore et al., 2018). In the adult CNS massive GABAergic activity led to a [Cl$^-$]$_i$ increase, which depends on HCO$_3^-$ gradients and additional [K$^+$]$_e$ transients (Staley et al., 1995; Kaila et al., 1997). However, there is little evidence that also moderate levels of GABAergic activity can mediate functionally relevant [Cl$^-$]$_i$ changes in the mature nervous system (Kaila et al., 1997). In contrast, already physiological levels of GABAergic activity affect [Cl$^-$]$_i$ the immature nervous system (Kolbaev et al., 2011b; Lombardi et al., 2018), in which the steady-state [Cl$^-$]$_i$ is high (Cherubini et al., 1991; Ben-Ari, 2002). These transient [Cl$^-$]$_i$ changes after limited GABAergic stimulation is most probably due to the low capacity of NKCC1-mediated Cl$^-$ accumulation in these neurons (Achilles et al., 2007). The activity-dependent [Cl$^-$]$_i$-decrease in the immature nervous system serves to limit the excitatory action of GABA (Ben-Ari et al., 2012; Kilb et al., 2013). But in the adult situation, the activity-dependent [Cl$^-$]$_i$ increase attenuates the inhibitory potential of GABA and, in case of a strong GABAergic activity, could even render GABA excitatory (Staley et al., 1995; Kaila et al., 2014b).

The activity-dependent [Cl$^-$]$_i$ changes depend on the activity of [Cl$^-$]$_i$ transport mechanisms, the conductance and distribution of Cl$^-$ channels, the diameter and topology of dendrites, as well as on distance of synaptic sites from the soma (Doyon et al., 2011; Jedlicka et al., 2011; Kaila et al., 2014a; Mohapatra et al., 2016; Lombardi et al.,

2019). Thus, activity-dependent [Cl$^-$]$_i$ changes are mainly restricted to the dendritic compartment (Doyon et al., 2011; Jedlicka et al., 2011). The amount of Cl$^-$ fluxes during a GABAergic event is determined by the difference between E$_m$ and E$_{Cl}$ [i.e., the driving force for Cl$^-$ (DF$_{Cl}$; Ballanyi and Grafe, 1985; Backus et al., 1998; Kuner and Augustine, 2000; Jedlicka and Backus, 2006]. Accordingly, stabilization of E$_m$ by a low input resistance (Lombardi et al., 2019) or a positive shift in E$_{GABA}$ due to the contribution of HCO$_3^-$ to GABAergic currents (Rivera et al., 2005; Wright et al., 2011; Lombardi et al., 2019) enhances the activity-dependent [Cl$^-$]$_i$ changes in neurons. Since the synchronous stimulation of glutamate receptors will depolarize E$_m$ and therefore enhance DF$_{Cl}$, a coincident activation of glutamate receptors will enhance the Cl$^-$ fluxes through GABA$_A$ receptors. While it has already been demonstrated that a depolarization indeed enhances GABAergic [Cl$^-$]$_i$ transients (Ballanyi and Grafe, 1985; Thompson and Gähwiler, 1989; Kuner and Augustine, 2000) and it is obvious that a massive glutamatergic stimulation will thus lead to larger [Cl$^-$]$_i$ transients (Moore et al., 2018), it has not been shown experimentally whether moderate levels of glutamatergic activity are indeed sufficient to substantially enhance GABAergic [Cl$^-$]$_i$ transients. In addition, it is currently unknown whether moderate levels of ionic plasticity in [Cl$^-$]$_i$ significantly affect GABAergic inhibition, although some studies demonstrate that massive GABAergic stimulation can render GABA excitatory via ionic plasticity (Staley et al., 1995; Fujiwara-Tsukamoto et al., 2003; Isomura et al., 2003).

To address the question, whether coincident activation of GABA$_A$ and glutamate receptors mediate increased ionic plasticity, we induced short trains of GABA$_A$ receptor activations, applied either with or without synchronous glutamatergic activation, and analyzed the resulting changes in [Cl$^-$]$_i$. To further investigate whether these [Cl$^-$]$_i$ changes lead to a functionally relevant reduction of inhibitory capacity, we additionally determined whether these stimulation paradigms change the GABAergic rheobase shift. These experiments revealed that GABAergic activity leads to a [Cl$^-$]$_i$ increase and attenuates the inhibitory effect of GABA. While coincident glutamate receptor activation augments the activity-dependent [Cl$^-$]$_i$ shifts, it does not have additional effect on the activity-induced decrease in GABAergic inhibitory capacity.

## MATERIALS AND METHODS

### Preparation of Dissociated Neuronal Cultures

Experiments were performed in primary cortical neurons cultured from newborn (postnatal day 0) mice (C57BL6). After decapitation brains were transferred to ice-cold Ca$^{2+}$- and Mg$^{2+}$-free HBSS (Gibco, Invitrogen, Carlsbad, CA, USA) supplemented with penicillin and streptomycin (50 units/ml), sodium pyruvate (11 mg/ml), glucose (0.1%), and HEPES (10 mM). Cortical cells were dissociated via trypsin incubation for 20 min at 37°C and DNAse digestion at room temperature

(RT). After blocking trypsinization by washing steps with HBSS, Minimal Essential Medium (MEM, Gibco) supplemented with 10% horse serum and 0.6% glucose was added. Next the cells were mechanically dissociated *via* repetitive pipetting through fire-polished glass pipettes with declining diameter. Following cell counting, cells were seeded on Polyornithine-coated glass coverslips in a 24-well-plate (density: 1,000 cells/mm$^2$). After 45 min, the medium was exchanged for medium consisting of Neurobasal medium (Gibco) supplemented with 2% B27 (Gibco) and 1 mM L-glutamine.

Cells were cultivated at 37°C in humidified carbogen (95% air; 5% $CO_2$) for up to 22 days. At 3 days *in vitro* (DIV) 5 μM AraC was added to the medium to inhibit glial cell proliferation. A quarter of the medium was exchanged weekly.

## rtPCR

Total RNA from primary cortical cultures was isolated using the RNeasy Mini Kit (Qiagen). mRNA was reverse transcribed using the Transcriptor High Fidelity cDNA Synthesis Kit (Roche Applied Science). qRT-PCR was performed using the LightCycler TaqMan Master Kits as well as probes and primers designed with the Universal Probe Library in a LightCycler 1.5 System (all Roche Applied Science). Primer sequences (in 5′–3′orientation) of target gene and probes are as follows: KCC2 (UPL probe #79), TTCGACCCACCCAATTTC and AAAGCCATGGCGAGACAG; β-actin (UPL probe#106), TGACAGGATGCAGAAGGAGA and CGCTCAGGAGGAGC-AATG. The qRT-PCR crossing points were used for relative quantification based on the ΔCt-method using the StepOne software (version 2.3) and β-actin was used as a reference gene (Pfaffl et al., 2002).

## Immunohistochemistry

Primary cortical neurons grown on coverslips were fixed in 4% PFA in PBS for 20 min after 7 or 14 days in culture. After washing with PBS unspecific binding of antibodies was blocked with 7% normal donkey serum and 0.3% Triton diluted in PBS for 2 h (RT). Overnight staining was performed at 4°C with rabbit anti-KCC2 antibody (Sigma Aldrich, #07-432) diluted 1:500 in 2% bovine serum albumin with 0.05% azide and 0.1% Triton. After subsequent wash with PBS, cells were incubated with DAPI and DyLight488-coupled secondary antibodies (Dianova and Biomol, Hamburg, Germany) diluted 1:500 in 2% bovine serum albumin with 0.05% azide in PBS at RT for 2 h. Coverslips were washed in PBS and specimens were mounted with Fluoromount (Sigma-Aldrich).

## MEA Recordings

Extracellular electrical recordings were performed as described previously (Weir et al., 2015). In short, cells were cultured on MEAs containing 120 planar extracellular titanium nitrite electrodes with four internal references (120MEA100/30iR-Ti-gr, Multi Channel Systems). MEAs had an electrode diameter of 30 μm and an interelectrode spacing of 100 or 200 μm. Signals from 120 recording electrodes were recorded with MC_Rack software in a MEA 2100 system (Multi Channel Systems) at a sampling rate of 50 kHz and high-pass filtered at 200 Hz. Spikes were detected using a negative threshold-based detector

set to a threshold of 7× the SD of the noise level (MC_Rack, Multi Channel Systems). Electrophysiological recordings were performed in artificial cerebrospinal fluid (ASCF) resembling the medium composition consisting of (in mM) 129 NaCl, 26 $NaHCO_3$, 1 $MgCl_2$, 2 $CaCl_2$, 5.3 KCl, 10 glucose (equilibrated with 95% $O_2$/5% $CO_2$). Temperature was maintained at 32°C by a temperature controller (TC02, Multi Channel Systems). Spike datasets from all electrodes recorded for 10 min were imported into Matlab 7.7 (Mathworks, Natick, MA, USA) for analysis of single units using a custom written routine. Spike sorting was carried out as described previously (Sun et al., 2010). Autocorrelation functions were applied to confirm spike sorting. If single units fired ≥2 times within the recording period, units were counted as active neurons. Average firing frequencies were calculated as arithmetic mean of individual firing frequencies of all identified units.

## Whole-Cell Patch-Clamp Recording

For patch-clamp experiments, cultured cells were transferred into ACSF that consisted of (in mM) 126 NaCl, 26 $NaHCO_3$, 1.25 $NaH_2PO_4$, 1 $MgCl_2$, 2 $CaCl_2$, 2.5 KCl, 10 glucose and was equilibrated with 95% $O_2$/5% $CO_2$ (pH = 7.4; osmolarity = 316 mOsm). In the experimental setup, cells were constantly perfused with ACSF at a rate of 2 ml/min. All experiments were performed at 31 ± 1°C.

Cell cultures were visualized using an inverted microscope (BX51WI, Olympus) equipped with a CCD camera (VX45, Optronics, Goleta, CA, USA) connected to a video monitor (PVM-145E, Sony). Pictures of each cell were taken to be able to reconstruct morphology and pipette positioning. Only cells with clearly visible dendritic extensions downstream the bath perfusion and facing the insertion site of the application pipettes were chosen to minimize steric problems while positioning the pipettes. The patch electrode, as well as one of the application pipettes, were positioned using electric manipulators (SM-1, Luigs and Neumann, Ratingen, Germany), while the second application pipette was mounted on manual manipulators. The application pipettes were positioned in the dendritic tree ~100 μm apart from the soma downstream the bath perfusion to make sure that no other cell compartments are superfused by the applied substances *via* the perfusion system. Muscimol (200 μM, 10 ms) and glutamate pulses (200 μM, 20 ms) were delivered by separate pipettes, while muscimol application for $E_{GABA}$ determination and burst like $GABA_A$ receptor activation was delivered *via* the same pipette. Focal application was conducted *via* a custom-built pressure application system (Lee, Westbrook, CT, USA) at a pressure of 0.5 bar. To impede the removal of focally applied neurotransmitter, an additional suction pipette was placed close to the application sites by a manual manipulator.

Patch-clamp recordings were conducted with a discontinuous voltage clamp/current clamp amplifier (SEC05L, NPI, Tamm, Germany), connected to a standard personal computer *via* a digital-analog converter (LIH1600, HEKA Electronics, Lambrecht, Germany). Both, recording data for later analysis and executing protocols were mediated by TIDA software (TIDA 5.25, HEKA). Patch electrodes and application pipettes were

pulled from borosilicate glass capillaries (GB200F-8, Science Products, Hofheim am Taunus, Germany) using a vertical electrode puller (Model PP-830, Narishige Co., Tokyo, Japan). For the majority of whole-cell recordings, the patch electrodes (resistance 3–5 MΩ) were filled with a K-gluconate based pipette solution containing 10 mM $Cl^-$ (128 K-gluconate, 4 KCl, 1 $CaCl_2$, 4 NaCl, 11 EGTA, 10 K-HEPES, pH adjusted to 7.4 with KOH and osmolarity to 300 mOsm with sucrose). Few control experiments were performed with a high $Cl^-$ pipette solution containing 20 mM $Cl^-$ (118 K-gluconate, 14 KCl, 1 $CaCl_2$, 4 NaCl, 11 EGTA, 10 K-HEPES, pH adjusted to 7.4 with KOH and osmolarity to 300 mOsm with sucrose) or 50 mM $Cl^-$ (88 K-gluconate, 44 KCl, 1 $CaCl_2$, 4 NaCl, 11 EGTA, 10 K-HEPES, pH adjusted to 7.4 with KOH and osmolarity to 300 mOsm with sucrose). All potentials were corrected for liquid junction potential of −14.4 mV for 10 mM $Cl^-$ solution, −13.5 for 20 mM $Cl^-$ solution and −10.7 mV for 50 mM $Cl^-$ solution.

To estimate $[Cl^-]_i$, the GABA reversal potential was determined by either muscimol applications (200 µM, 10 ms) at different holding potentials (−80, −60 and −40 mV) or by paired voltage ramps (−80 to −20 mV; 50 ms; 2 V/s), one applied at control conditions and a second during the peak of a muscimol response, induced by a single application of muscimol (**Figures 2A,B**). To minimize the influence of these muscimol induced currents on $[Cl^-]_i$, we only used three muscimol pulses at holding potentials between −80 and −40 mV. $E_{GABA}$ was estimated either from the intersection of the linear fit with the abscissa for voltage step determination and from the intersection of the control voltage ramp response and the voltage ramp response during muscimol peak (**Figure 2C**). $[Cl^-]_i$ was calculated from $E_{GABA}$ using the Nernst equation. The experiments with voltage-ramp $E_{GABA}$ determination were performed with 0.1 µM TTX to prevent AP generation by the voltage ramps and reduce spontaneous activity. Spontaneous excitatory (EPSCs) and inhibitory postsynaptic currents (IPSCs) were recorded with a 10 mM $[Cl^-]_p$, were isolated by their reversal potential, and were analyzed with Minianalysis software (Synaptosoft, Fort Lee, NY, USA).

For "burst-like" focal application, a train of 10 single pulses at a frequency of 10 Hz was applied at a holding potential of −60 mV in current-clamp mode. In few control experiments, cells were voltage-clamped during the burst-like focal application. The slope of $[Cl^-]_i$ back regulation was determined by fitting the $[Cl^-]_i$ decay with a monoexponential function and calculating the apparent $[Cl^-]_i$ changes between the arbitrary $[Cl^-]_i$ values of 17.5 mM and 18.5 mM (**Figure 3D**). The rheobase [i.e., the minimal injection current required to trigger action potentials (AP)] and the muscimol-induced rheobase shift were determined using paired current ramps of 50 ms duration with 2 nA maximum current and separated by a 1 s interval and applied a muscimol pulse (200 µM, 10 ms) during the second ramp. Muscimol application was temporally aligned to the voltage ramp for each cell separately, to obtain conditions where the current ramp is delivered during the peak of the muscimol response (Kolbaev et al., 2011a). Using this protocol, the rheobase for the first ($I_{RB}^{ctrl}$) and the second ($I_{RB}^{GABA}$)

current ramp was determined and the relative rheobase shift ($\Delta I_{RB} = I_{RB}^{muscimol} - I_{RB}^{ctrl}$) was calculated (see **Figure 6A**). $I_{RB}^{ctrl}$ was used to determine whether repetitive GABAergic inputs affect the excitability of the cell.

## Statistics

All data are presented as mean ± SEM. Statistical significance was determined using Student's $t$-test. Results were designated significant at a level of $p < 0.05$ and significance levels are $*p < 0.05$, $**p < 0.01$, and $***p < 0.001$. Significance of multiple comparisons was calculated with one-way ANOVA followed by or repeated-measure ANOVA followed by Bonferroni corrected *post hoc* tests (SPSS, IBM).

## RESULTS

## Stable Inhibitory Responses Are Established in Dissociated Neuronal Cultures at DIV13

In a first set of control experiments, we identified the time point at which stable inhibitory GABAergic responses are established in dissociated cell cultures under our experimental conditions. Quantitative rtPCR experiments revealed that the relative levels of KCC2 mRNA in primary neurons increased significantly ($p = 0.026$) from 0.008 ± 0.002 at DIV 7 ($n = 16$ replicates from eight cultures) to 0.016 ± 0.003 ($n = 15$ replicates from eight cultures) at DIV14 (**Figure 1A**). This upregulation of KCC2 mRNA is also visible by increased immunohistochemical labeling of neurons with KCC2 specific antibodies between DIV7 and DIV14 (**Figure 1B**), illustrating that also protein levels of KCC2 are upregulated. This KCC2 upregulation was paralleled by the establishment of inhibitory GABAergic responses in dissociated cell cultures, as analyzed in recordings with planar MEAs. The baseline firing frequency of cultured cortical neurons was 0.14 ± 0.03 Hz ($n = 74$ neurons from six cultures) at DIV6–8, which significantly ($p = 6.2*10^{-5}$) increased to 0.38 ± 0.03 Hz ($n = 218$ neurons from seven cultures) at DIV13–15 (**Figures 1C–E**), illustrating the typical developmental up-regulation of network connectivity (Wagenaar et al., 2006; Sun et al., 2010). Inhibition of $GABA_A$ receptors by 20 µM gabazine decreased the firing frequency in DIV 6–8 cultures by 69.4 ± 10.6% ($n = 64$ neurons from six cultures), indicating an excitatory effect of $GABA_A$ receptors at this developmental stage (**Figures 1C,F**). In contrast, at DIV13–15 gabazine application increased the firing frequency to 115.8 ± 58.8% ($n = 271$ neurons from seven cultures), suggesting that $GABA_A$ receptors mediate an inhibitory effect (**Figures 1D,F**).

In summary, these results indicate that cortical cultures older than DIV13 show the typical inhibitory GABAergic properties that are characteristic for mature neurons. Therefore, all further experiments were performed at DIV 13–18.

## Repetitive $GABA_A$ Receptor Activation Induces Short-Lasting $[Cl^-]_i$ Transients

To limit the variability in the $[Cl^-]_i$, we decided to use whole-cell patch-clamp recordings to stabilize $[Cl^-]_i$ by diffusional
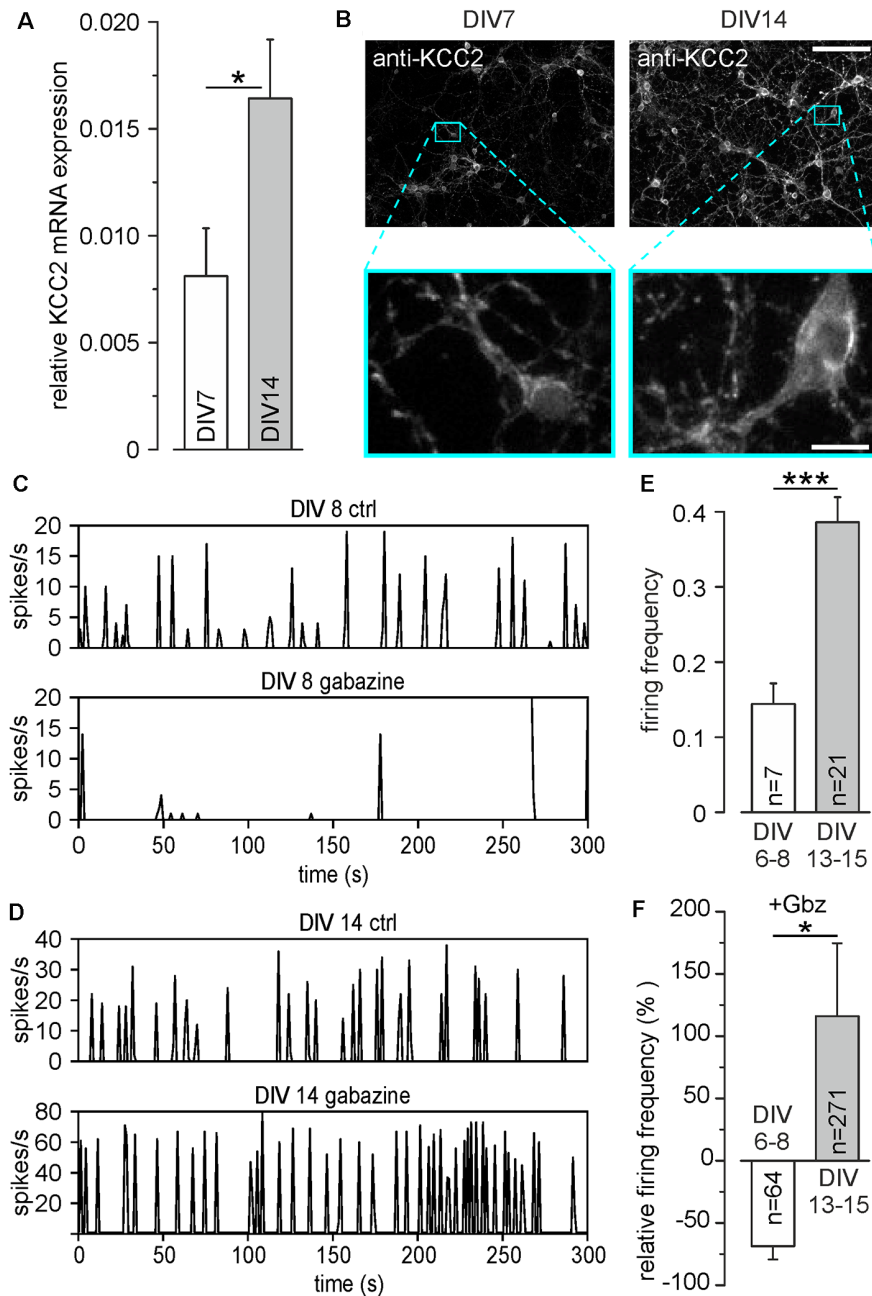
**FIGURE 1 |** Development of inhibitory γ-amino butyric acid (GABA) responses in dissociated cell cultures during the first 15 DIV. **(A)** Relative mRNA levels of potassium chloride cotransporter 2 (KCC2) at different days *in vitro* (DIV). **(B)** Antibody staining against KCC2 at DIV 7 and DIV14. The lower panels show a 10× magnification of the marked areas in the upper panels. Note the strong increase of KCC2 expression, especially in dendritic compartments. Scale bars: 100 μm (upper panels); 10 μm (lower panels). **(C)** Representative MEA recordings at DIV 8 under control conditions and in the presence of 20 μM gabazine. **(D)** Representative MEA recordings at DIV 14 under control conditions and in the presence of 20 μM gabazine. **(E)** Average firing frequency of all units recorded on MEAs, measured at DIV 6–8 and DIV 13–15, respectively. Note that compared to DIV 6–8, the average firing frequency was significantly increased at DIV 13–15. **(F)** Effect of the GABA receptor antagonist gabazine (Gbz, 20 μM) on firing frequency. Gabazine decreased the firing frequency at DIV 6–8, while it led to an increase at DIV 13–15. Bars represent mean ± SEM, *, ***indicate significance levels of $p < 0.05$ and $p < 0.001$, respectively.

exchange with the pipette solution (Pusch and Neher, 1988). In order to demonstrate that this approach will still allow us to detect dynamic $[Cl^-]_i$ changes in the dendrite (Jarolimek et al., 1999), we used a rather high $[Cl^-]_p$ of 20 mM to challenge the

$Cl^-$ extrusion within the dendritic compartment. To verify that $[Cl^-]_i$ is not clamped in the dendrite, we determined $E_{Cl}$ by a voltage ramp protocol (**Figures 2A–C**) using focal muscimol application at the soma and at the dendrite ~100 μm apart from

**FIGURE 2 |** Determination of somatic and dendritic $[Cl^-]_i$ in whole-cell patch-clamp experiments. **(A)** Typical current traces upon injection of voltage ramps which are used to determine $E_{Cl}$. The second voltage ramp was applied during the peak of a muscimol response. **(B)** Voltage ramp and current response is shown in **(A)** at higher temporal resolution. Note the divergent current amplitude in the presence of muscimol (red trance). **(C)** Relation between muscimol-dependent current difference ($\Delta I = I_{Muscimol} - I_{Baseline}$) and the holding potential ($V_H$). $E_{rev}$ was determined from a linear fit between 14 and 44 ms. **(D)** Brightfield pictures of a r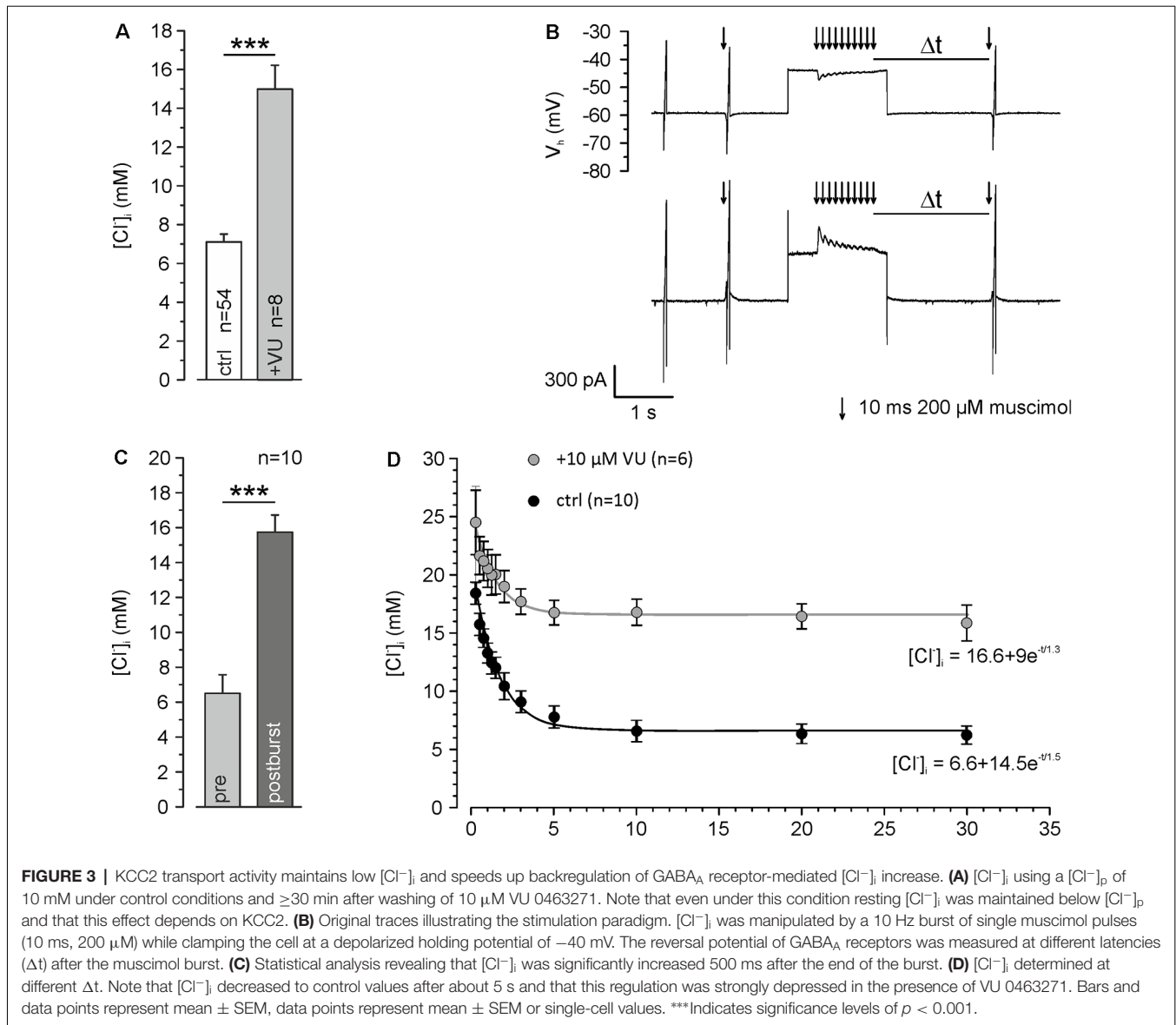ecorded cell illustrating application pipettes positioned near the soma (upper panel) and at the dendrite (lower panel). Scale bar: 50 µm. **(E)** Resting $[Cl^-]_i$ at the soma compared to a dendritic compartment 100 µm apart from the soma center. All experiments were performed under whole-cell conditions with a pipette solution containing 20 mM $Cl^-$ ($[Cl^-]_p$). Note the significant lower $[Cl^-]_i$ in the dendrite. **(F)** Time course of dendritic $E_{rev}$ after inhibition of KCC2 with 10 µM VU 0463271. Note the strong $[Cl^-]_i$ increase upon KCC2 inhibition. **(G)** Dendritic $[Cl^-]_i$ at rest and after VU 0463271 application ($\geq$30 min). Note that VU 0463271 induced a significant increase in $[Cl^-]_i$. Bars/data points represent mean $\pm$ SEM. *,***Indicate significance levels of $p < 0.05$ and $p < 0.001$, respectively.

the soma (**Figure 2D**). We measured a mean somatic $[Cl^-]_i$ of $17.6 \pm 0.7$ mM ($n = 10$ neurons from six cultures) and a significantly ($p = 0.03$) lower dendritic $[Cl^-]_i$ of $15.4 \pm 1.3$ mM ($n = 10$ neurons from six cultures; **Figure 2E**), indicating that $Cl^-$-extrusion is capable to partially control dendritic $[Cl^-]_i$. Inhibition of $Cl^-$-extrusion with the KCC2 antagonist VU 0463271 (10 µM; Sivakumaran et al., 2015) induced an increase in dendritic $[Cl^-]_i$ (**Figure 2F**). The dendritic $[Cl^-]_i$ significantly ($p = 1.6*10^{-5}$) increased from $15.4 \pm 1.3$ mM ($n = 10$ neurons from six cultures) to $25.8 \pm 1.3$ mM ($n = 12$ neurons from five cultures) after VU 0463271 application (**Figure 2G**). These experiments indicate a substantial $[Cl^-]_i$ gradient in the dendrite that was maintained by KCC2 activity (Jarolimek et al., 1999).

All further experiments are performed under whole-cell condition using a $[Cl^-]_p$ of 10 mM, to match the estimated $[Cl^-]_i$ of mature neurons. Under these conditions, the dendritic $[Cl^-]_i$ is maintained at $7.0 \pm 0.4$ mM ($n = 54$ neurons from 46 cultures). These values increased to $15.0 \pm 1.2$ mM ($n = 8$ neurons from five cultures) after treatment with 10 µM VU 0463271 (**Figure 3A**), again indicating the important role of KCC2 for dendritic $[Cl^-]_i$ homeostasis. To reveal the kinetics of KCC2-dependent $[Cl^-]_i$ regulation in the dendritic compartment, we repeatedly induced a $[Cl^-]_i$ shift by burst application ($10 \times 10$ ms at 10 Hz) of 200 µM muscimol at a slightly depolarized $V_H$ of $-40$ mV and determined $E_{Cl}$ at different time points after the muscimol burst application (**Figure 3B**). The muscimol burst application induced a $[Cl^-]_i$ increase from $6.5 \pm 1.1$ mM to $15.7 \pm 1.0$ mM ($n = 10$ neurons from eight cultures; **Figure 3C**), as determined at 500 ms after the burst. This $[Cl^-]_i$ increase was regulated back to baseline levels of $6.2 \pm 0.8$ mM within several seconds (**Figure 3D**). The slope of $[Cl^-]_i$ backregulation amounted to $-9.6$ mM/s. In the presence of 10 µM VU 0463271 the backregulation after
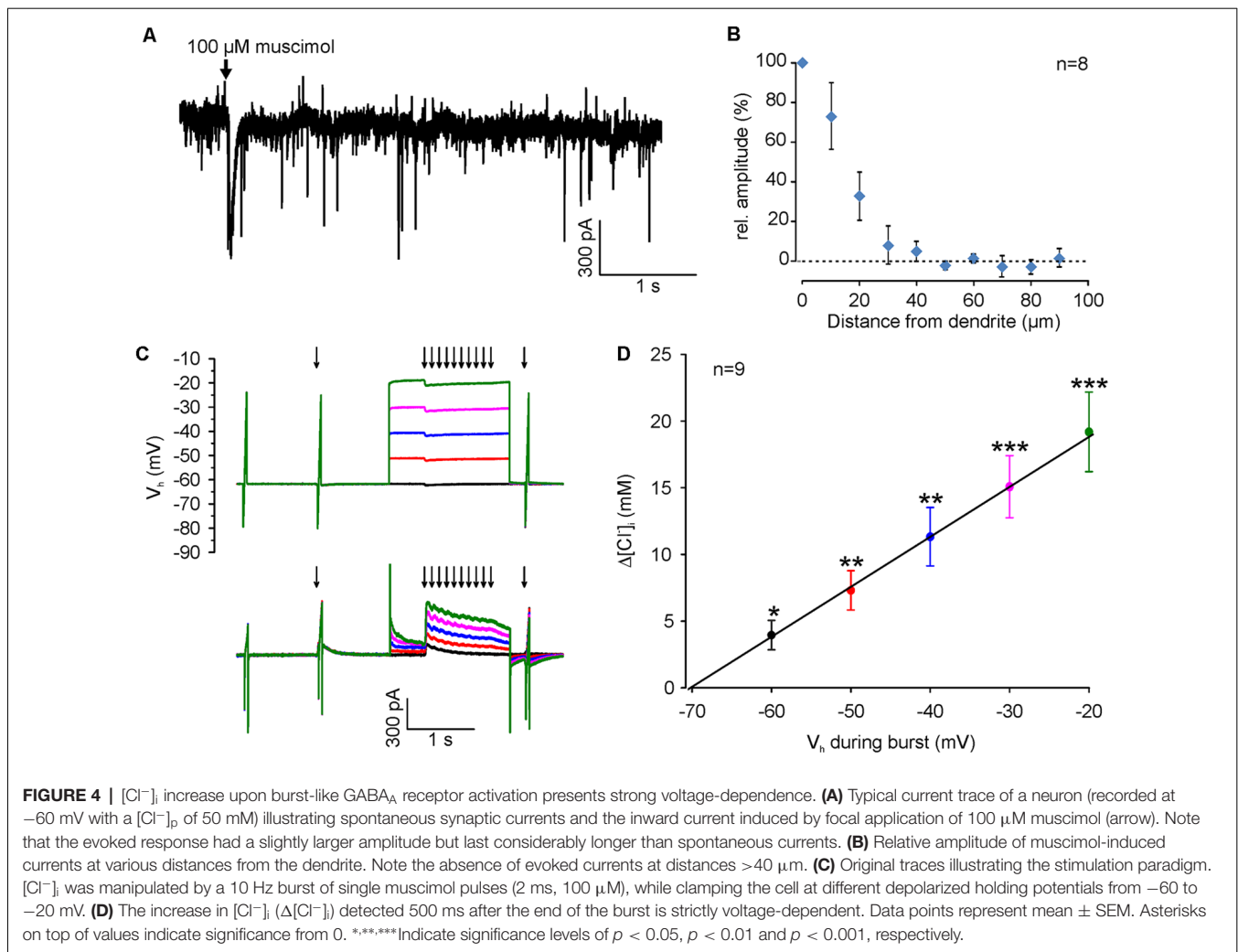
**FIGURE 3** | KCC2 transport activity maintains low $[Cl^-]_i$ and speeds up backregulation of GABA$_A$ receptor-mediated $[Cl^-]_i$ increase. **(A)** $[Cl^-]_i$ using a $[Cl^-]_p$ of 10 mM under control conditions and $\geq$30 min after washing of 10 $\mu$M VU 0463271. Note that even under this condition resting $[Cl^-]_i$ was maintained below $[Cl^-]_p$ and that this effect depends on KCC2. **(B)** Original traces illustrating the stimulation paradigm. $[Cl^-]_i$ was manipulated by a 10 Hz burst of single muscimol pulses (10 ms, 200 $\mu$M) while clamping the cell at a depolarized holding potential of $-40$ mV. The reversal potential of GABA$_A$ receptors was measured at different latencies ($\Delta$t) after the muscimol burst. **(C)** Statistical analysis revealing that $[Cl^-]_i$ was significantly increased 500 ms after the end of the burst. **(D)** $[Cl^-]_i$ determined at different $\Delta$t. Note that $[Cl^-]_i$ decreased to control values after about 5 s and that this regulation was strongly depressed in the presence of VU 0463271. Bars and data points represent mean $\pm$ SEM, data points represent mean $\pm$ SEM or single-cell values. ***Indicates significance levels of $p < 0.001$.

muscimol burst application was slowed down to $-1.0$ mM/s and reached steady-state values at 15.9 $\pm$ 1.5 mM ($n = 6$ neurons from five cultures; **Figure 3D**), demonstrating the essential role of KCC2 for efficient $[Cl^-]_i$ homeostasis within the dendritic compartment.

In summary, these experiments show that dendritic muscimol bursts induce short-lasting $[Cl^-]_i$ transients even under whole-cell conditions and that KCC2 maintains the resting $[Cl^-]_i$ and determines the fast temporal properties of $[Cl^-]_i$ homeostasis.

## GABA$_A$ Receptor-Mediated $[Cl^-]_i$ Transients Are Voltage-Dependent

Since we attempted to use moderate stimulation conditions that are close to physiological levels of GABAergic activity, we limited the muscimol pulses by a fast application system

with an efficient local removal. With this system the focal application of muscimol (100 $\mu$M, 10 ms) induced a current of 65.4 $\pm$ 9.2 pA ($n = 13$ neurons from six cultures), which is only about 2$\times$ larger than spontaneous GABAergic IPSCs (31.2 $\pm$ 0.3 pA, $n = 5157$ events from four neurons; **Figure 4A**). In addition, the local removal system limited the spatial dimension of the GABAergic stimulation to $<40$ $\mu$M (**Figure 4B**), indicating that only a fraction of the dendrite was stimulated. To study the question, whether coincident depolarization by glutamate receptors can in principle affect ionic plasticity upon GABA$_A$ receptor activation, we first investigated how E$_m$ during muscimol burst application (10 $\times$ 10 ms pulses of 100–200 $\mu$M muscimol at 10 Hz), influences muscimol-induced $[Cl^-]_i$ transients in dendrites (**Figure 4C**). These experiments demonstrated a significant $[(F_{(4,32)} = 39.38)$, $p < 0.001$, repeated-measure ANOVA] linear
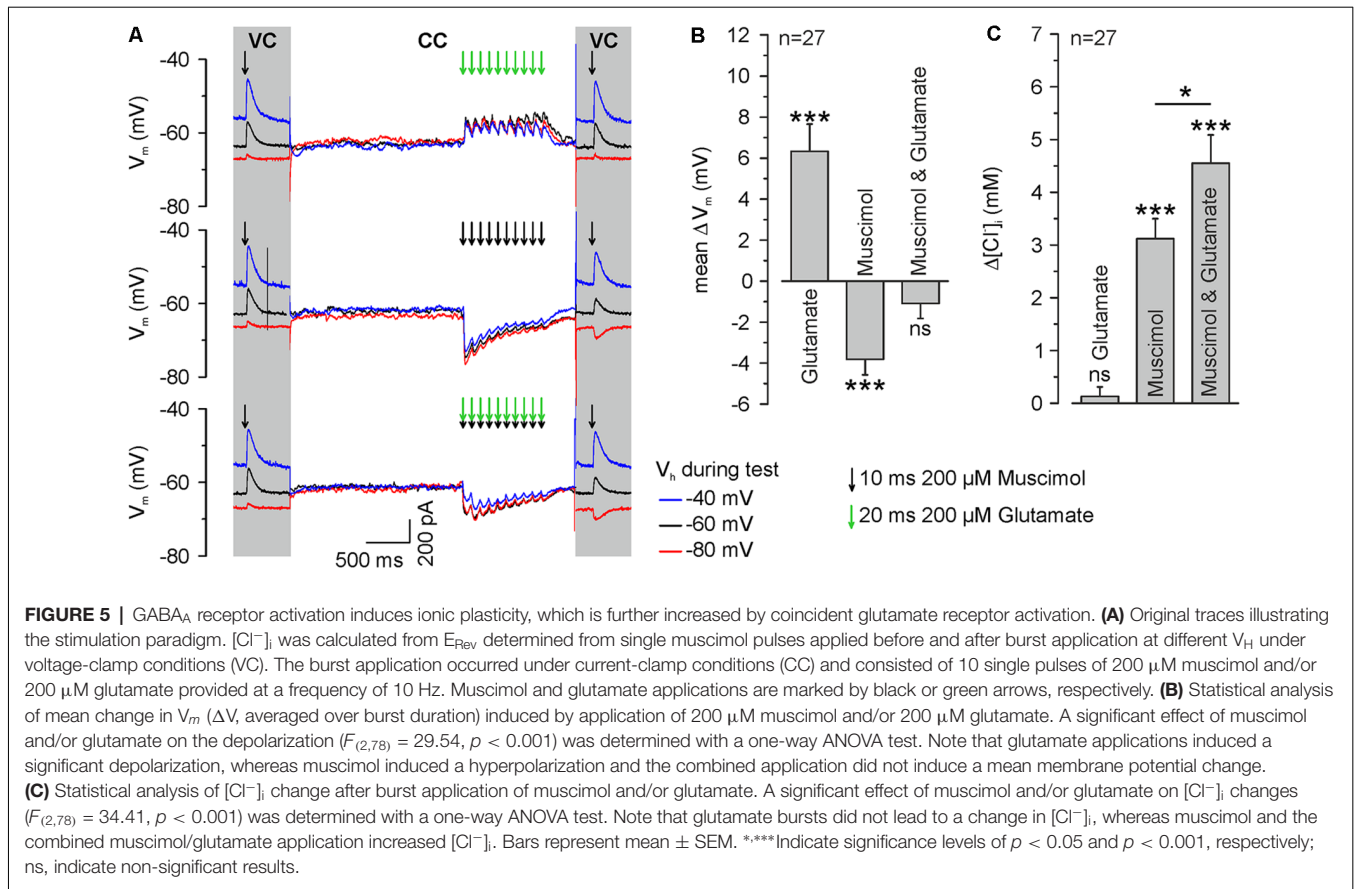
**FIGURE 4 |** [$Cl^-$]$_i$ increase upon burst-like $GABA_A$ receptor activation presents strong voltage-dependence. **(A)** Typical current trace of a neuron (recorded at −60 mV with a [$Cl^-$]$_p$ of 50 mM) illustrating spontaneous synaptic currents and the inward current induced by focal application of 100 μM muscimol (arrow). Note that the evoked response had a slightly larger amplitude but last considerably longer than spontaneous currents. **(B)** Relative amplitude of muscimol-induced currents at various distances from the dendrite. Note the absence of evoked currents at distances >40 μm. **(C)** Original traces illustrating the stimulation paradigm. [$Cl^-$]$_i$ was manipulated by a 10 Hz burst of single muscimol pulses (2 ms, 100 μM), while clamping the cell at different depolarized holding potentials from −60 to −20 mV. **(D)** The increase in [$Cl^-$]$_i$ ($\Delta$[$Cl^-$]$_i$) detected 500 ms after the end of the burst is strictly voltage-dependent. Data points represent mean ± SEM. Asterisks on top of values indicate significance from 0. *,**,***Indicate significance levels of $p < 0.05$, $p < 0.01$ and $p < 0.001$, respectively.

dependence between the observed [$Cl^-$]$_i$ shifts ($\Delta$[$Cl^-$]$_i$) and the membrane potential during $GABA_A$ receptor activation (3.8 ± 1 mM at $V_H$ of −60 mV; 7 ± 1.3 mM at −50 mV; 10.7 ± 2 mM at −40 mV; 14.2 ± 2.1 mM at −30 mV; 18 ± 2.7 mM at −20 mV; $n$ = 9 neurons; **Figure 4D**). This result replicates previous observations (Thompson and Gähwiler, 1989; Backus et al., 1998; Kuner and Augustine, 2000) and indicates that $GABA_A$ receptor-mediated [$Cl^-$]$_i$ transients can act as coincidence detectors for synchronous depolarizations.

## Coactivation of Glutamate Receptors Augments $GABA_A$ Receptor-Mediated [$Cl^-$]$_i$ Transients

To directly address our central question whether a glutamatergic coactivation can augment $GABA_A$ receptor-mediated [$Cl^-$]$_i$ transients, we next applied glutamate in a burst-like pattern (10 × 20 ms pulses of 200 μM glutamate at 10 Hz) at identical time points to the muscimol burst application. These burst-like applications of glutamate were performed *via* a

pipette located close to the muscimol pipette at the dendrite under current-clamp conditions to allow the cell membrane to integrate GABAergic and glutamatergic postsynaptic potentials. The amplitude of focal glutamate pulses (37.8 ± 9.5 pA, $n$ = 11 neurons from six cultures) was comparable to the amplitude of spontaneous glutamatergic EPSCs (39.7 ± 0.5 pA, $n$ = 5,273 events from four neurons). Subsequently, [$Cl^-$]$_i$ was determined from a muscimol application under voltage-clamp conditions using a step protocol (**Figure 5A**).

These experiments demonstrated that a burst of 10 glutamate applications induced a mean depolarization of 7 ± 1.4 mV ($n$ = 27 neurons), whereas burst-like application of 10 muscimol pulses induced a mean hyperpolarization of −3.7 ± 0.2 mV ($n$ = 27 neurons). When both substances were applied simultaneously, $E_m$ remained mostly unaffected (−0.8 ± 0.7 mV, $n$ = 27; **Figure 5B**), indicating that glutamate co-application substantially affects the driving force on $Cl^-$ ions ($DF_{Cl}$). Subsequent [$Cl^-$]$_i$ measurements (**Figure 5A**) revealed that a burst of 10 glutamate pulses, as expected, did not affect [$Cl^-$]$_i$ ($\Delta$[$Cl^-$]$_i$ = 0.1 ± 0.2 mM, $n$ = 27 neurons). Application of a burst of 10 muscimol pulses significantly ($p = 0.025$) increased

**FIGURE 5 |** GABA$_A$ receptor activation induces ionic plasticity, which is further increased by coincident glutamate receptor activation. **(A)** Original traces illustrating the stimulation paradigm. [Cl$^-$]$_i$ was calculated from E$_{Rev}$ determined from single muscimol pulses applied before and after burst application at different V$_H$ under voltage-clamp conditions (VC). The burst application occurred under current-clamp conditions (CC) and consisted of 10 single pulses of 200 µM muscimol and/or 200 µM glutamate provided at a frequency of 10 Hz. Muscimol and glutamate applications are marked by black or green arrows, respectively. **(B)** Statistical analysis of mean change in V$_m$ (ΔV, averaged over burst duration) induced by application of 200 µM muscimol and/or 200 µM glutamate. A significant effect of muscimol and/or glutamate on the depolarization ($F_{(2,78)}$ = 29.54, $p < 0.001$) was determined with a one-way ANOVA test. Note that glutamate applications induced a significant depolarization, whereas muscimol induced a hyperpolarization and the combined application did not induce a mean membrane potential change. **(C)** Statistical analysis of [Cl$^-$]$_i$ change after burst application of muscimol and/or glutamate. A significant effect of muscimol and/or glutamate on [Cl$^-$]$_i$ changes ($F_{(2,78)}$ = 34.41, $p < 0.001$) was determined with a one-way ANOVA test. Note that glutamate bursts did not lead to a change in [Cl$^-$]$_i$, whereas muscimol and the combined muscimol/glutamate application increased [Cl$^-$]$_i$. Bars represent mean ± SEM. *,***Indicate significance levels of $p < 0.05$ and $p < 0.001$, respectively; ns, indicate non-significant results.

[Cl$^-$]$_i$ by 3.1 ± 0.4 mM ($n$ = 27 neurons). Synchronous application of muscimol and glutamate led to a [Cl$^-$]$_i$ increase of 4.55 ± 0.53 mM ($n$ = 27 neurons; $p$ = 4.8*10$^{-4}$; **Figure 5C**), which is significantly ($p$ = 0.042) higher than the [Cl$^-$]$_i$ transient observed upon only muscimol pulses.
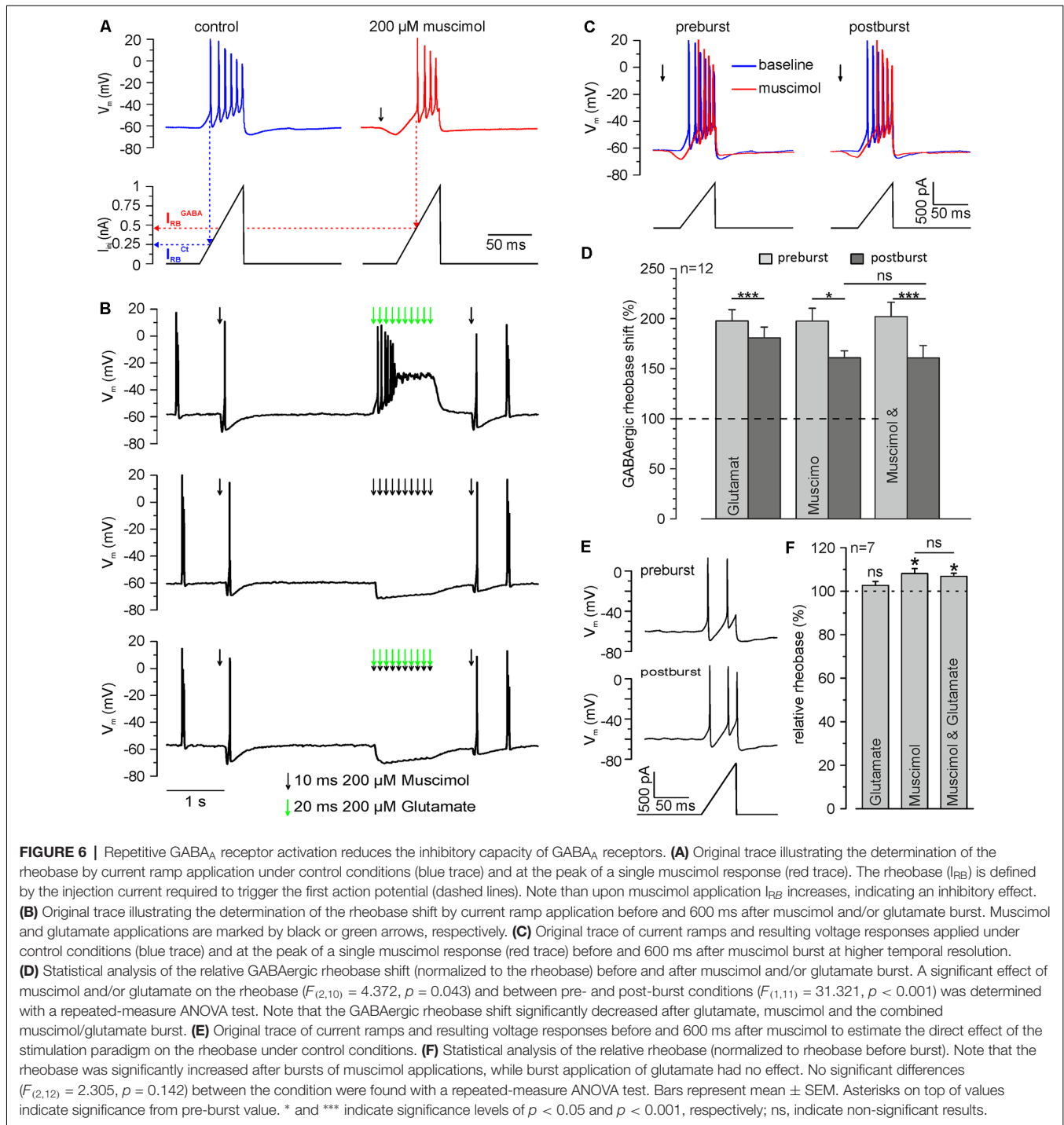
In summary, these results indicate that brief trains of GABAergic inputs induce substantial changes in [Cl$^-$]$_i$ and that these activity-dependent [Cl$^-$]$_i$ transients are augmented by glutamate coapplication, suggesting that activity-dependent [Cl$^-$]$_i$ changes can act as sort of coincidence detector for glutamatergic and GABAergic synaptic inputs.

## GABA$_A$ Receptor-Mediated [Cl$^-$]$_i$ Transients Cause a Reduction of GABAergic Inhibitory Capacity

Finally, we investigated if this [Cl$^-$]$_i$ increase results in a functionally relevant reduction of the inhibitory capacity mediated by GABA$_A$ receptors. In these experiments, we quantified the inhibitory capacity of GABA$_A$ receptors as GABAergic rheobase shift. For that purpose, we determined the rheobase (I$_{RB}$), i.e., the threshold current to evoke an AP, from a ramp-like current protocol. An inhibitory effect will require larger currents to reach AP threshold, thus increasing I$_{RB}$. We determined I$_{RB}$ under control conditions (I$_{RB}$$^{Ctrl}$) and in the presence of muscimol (I$_{RB}$$^{GABA}$), which allows us to quantify the

inhibitory capacity provided by GABA$_A$ receptors (**Figure 6A**). Upon application of a muscimol pulse, I$_{RB}$ increased significantly ($p$ = 2.1*10$^{-5}$) from 364.7 ± 25.5 pA to 721.9 ± 67.2 pA ($n$ = 12 neurons) corresponding to a GABAergic rheobase shift (I$_{RB}$$^{GABA}$ − I$_{RB}$$^{Ctrl}$) by 197.5 ± 12.8%. This finding indicates that activation of GABA receptors promotes a substantial inhibitory effect on the excitability of neurons. Next, we determined whether a burst-application of 10 muscimol pulses affects GABAergic rheobase shift, i.e., the inhibitory effect of GABA (**Figures 6B,C**). Burst application of 10 muscimol pulses induced a significant ($p$ = 0.033) reduction in the GABAergic rheobase shift from 197.5 ± 12.8 to 160.9 ± 8.7% ($n$ = 12 neurons; **Figure 6D**). When the burst-like application of muscimol was paired with coincident glutamate applications, the GABAergic rheobase shift decreased significantly ($p$ = 5.4*10$^{-4}$) from 201.9 ± 14.5% to 160.8 ± 12.3% ($n$ = 12 neurons; **Figure 6D**), which is not significantly different from the application of muscimol alone ($p$ = 0.98). Determination of the rheobase after a burst of 10 glutamate applications demonstrated significantly smaller ($p$ = 0.037) decrease of the GABAergic rheobase shift from 197.6 ± 11.2% to 180.7 ± 10.8% ($n$ = 12 neurons, $p$ = 3.3*10$^{-4}$; **Figure 6D**).

In order to exclude that a direct effect of either membrane potential alterations or the GABA$_A$ receptor-dependent [Cl$^-$]$_i$ changes on I$_{RB}$ (Sørensen et al., 2017) contributed to the observed reduction in the GABAergic rheobase shift, we also analyzed

**FIGURE 6 |** Repetitive GABA$_A$ receptor activation reduces the inhibitory capacity of GABA$_A$ receptors. **(A)** Original trace illustrating the determination of the rheobase by current ramp application under control conditions (blue trace) and at the peak of a single muscimol response (red trace). The rheobase (I$_{RB}$) is defined by the injection current required to trigger the first action potential (dashed lines). Note than upon muscimol application I$_{RB}$ increases, indicating an inhibitory effect. **(B)** Original trace illustrating the determination of the rheobase shift by current ramp application before and 600 ms after muscimol and/or glutamate burst. Muscimol and glutamate applications are marked by black or green arrows, respectively. **(C)** Original trace of current ramps and resulting voltage responses applied under control conditions (blue trace) and at the peak of a single muscimol response (red trace) before and 600 ms after muscimol burst at higher temporal resolution. **(D)** Statistical analysis of the relative GABAergic rheobase shift (normalized to the rheobase) before and after muscimol and/or glutamate burst. A significant effect of muscimol and/or glutamate on the rheobase ($F_{(2,10)}$ = 4.372, $p$ = 0.043) and between pre- and post-burst conditions ($F_{(1,11)}$ = 31.321, $p < 0.001$) was determined with a repeated-measure ANOVA test. Note that the GABAergic rheobase shift significantly decreased after glutamate, muscimol and the combined muscimol/glutamate burst. **(E)** Original trace of current ramps and resulting voltage responses before and 600 ms after muscimol to estimate the direct effect of the stimulation paradigm on the rheobase under control conditions. **(F)** Statistical analysis of the relative rheobase (normalized to rheobase before burst). Note that the rheobase was significantly increased after bursts of muscimol applications, while burst application of glutamate had no effect. No significant differences ($F_{(2,12)}$ = 2.305, $p$ = 0.142) between the condition were found with a repeated-measure ANOVA test. Bars represent mean ± SEM. Asterisks on top of values indicate significance from pre-burst value. * and *** indicate significance levels of $p < 0.05$ and $p < 0.001$, respectively; ns, indicate non-significant results.

I$_{RB}$$^{Ctrl}$ before and after the burst-like application protocol. We found that I$_{RB}$$^{Ctrl}$ was significantly ($p$ = 0.0119) increased by 8.1 ± 2.3% ($n$ = 7 neurons) after burst-like application of muscimol, as compared to values before burst application (**Figures 6E,F**). The combined burst application of muscimol and glutamate induced a significant ($p$ = 0.0128) increase in the I$_{RB}$$^{Ctrl}$ by 6.8 ± 1.4% ($n$ = 7 neurons), which is not significantly ($p$ = 0.55) different from burst-like muscimol application.

Burst-like application of only glutamate had no significant ($p$ = 0.35) effect on I$_{RB}$$^{Ctrl}$ (102.6 ± 1.8%; $n$ = 7 neurons). These experiments show that burst-like application of muscimol results in a small increase in the rheobase, which can have only a negligible contribution to the observed GABAergic rheobase shift under these conditions.

In summary, these results indicate that brief trains of GABAergic inputs induce a substantial reduction in the

GABAergic inhibitory capacity. However, an additional effect of coincident glutamate applications could not be observed.

## DISCUSSION

We used whole-cell patch-clamp recordings of cortical neurons in primary culture to analyze the effect of repetitive $GABA_A$ receptor activation on $[Cl^-]_i$ and the inhibitory capacity of $GABA_A$ receptors, particularly considering a modulation of these effects by coincident glutamate receptor activation. These experiments revealed, that: (i) considerable $[Cl^-]_i$ shifts could be induced by application of 10 GABAergic pulses under whole-cell conditions; (ii) that this GABA-induced $[Cl^-]_i$ transients were augmented at depolarized membrane potentials; (iii) that synchronous glutamate-applications augment the GABA-induced $[Cl^-]_i$ transients; (iv) that the GABA-induced $[Cl^-]_i$ transients decreased the inhibitory potential of GABA, but that (v) the synchronous coapplication of glutamate pulses had no additional effect on the attenuation of the inhibitory potential of GABA. In summary, these results indicate that moderate GABAergic stimulation induces transient and functionally relevant $[Cl^-]_i$ changes, which can be enhanced by coincident glutamatergic input.

We performed the experiments in neuronal cultures that were cultivated for at least 13 days, as neurons in these cultures display increased KCC2 expression and stable inhibitory GABAergic effects. The development of GABAergic inhibition during maturation *in vitro* is comparable to previous observations of $[Cl^-]_i$ and KCC2 expression in dissociated neuronal cultures (Kuner and Augustine, 2000; Ganguly et al., 2001; Titz et al., 2003). Although dissociated neuronal cultures differ in their synaptic connectivity from those *in vivo*, we decided to use this reduced preparation because it allows us to perform a spatially concise and selective activation of $GABA_A$ and/or glutamate receptors at a defined position in the dendrite. By using a local suction system to limit the spatial and temporal extent of the focal pressure application and by using rather short muscimol and or glutamate pulses, we were able to apply moderate GABAergic and glutamatergic stimuli. However, while the amplitudes of currents induced by focal muscimol or glutamate application are maximally two-fold larger than the average amplitudes of spontaneous synaptic currents, it must be emphasized that the focal pressure application does not represent physiological synapse-like stimulation. On one hand, the duration of the focal neurotransmitter applications is considerably longer than spontaneous PSCs and on the other hand, the spatial extent of the applied neurotransmitter spans about 40 $\mu$sm, thereby also activating extrasynaptic receptors.

Although the $[Cl^-]_i$ is in general tightly controlled by diffusional exchange with the pipette solution (Pusch and Neher, 1988), our whole-cell patch-clamp experiments revealed that the dendritic $[Cl^-]_i$ was substantially different from the somatic $[Cl^-]_i$, as had been demonstrated previously (Jarolimek et al., 1999; Moore et al., 2018). While the somatic $[Cl^-]_i$ was close to the $[Cl^-]_p$ for $[Cl^-]_p$ values of 10 mM or 20 mM, the dendritic $[Cl^-]_i$ levels were

significantly smaller under both conditions. The observation that this somato-dendritic $[Cl^-]_i$ gradient was abolished in the presence of VU0463271 indicates that it depends on KCC2 activity (Moore et al., 2018). In addition, substantial $[Cl^-]_i$ transients could be induced by repetitive muscimol pulses. These observations strongly suggest that the dendritic $[Cl^-]_i$ was only partially affected by the $[Cl^-]_p$. Therefore, we decided to perform all further experiments under whole-cell conditions instead of gramicidin-perforated patch conditions (Ebihara et al., 1995; Kyrozis and Reichling, 1995), as the whole-cell configuration allows more precise electrical control and also allows us to perform the experiments at more defined initial $[Cl^-]_i$. Although such whole-cell experiments may underestimate the real GABA-induced dendritic $[Cl^-]_i$ transients, our observation that the fast recovery of GABA-induced $[Cl^-]_i$ transients was abolished by the KCC2 inhibitor VU0463271 strongly suggests that the down-regulation of dendritic $[Cl^-]_i$ was dominated by transmembrane, KCC2-dependent $Cl^-$-transport. Diffusional exchange with the soma (Lombardi et al., 2019), and thus a putative contribution of somatic $[Cl^-]_i$ clamped by the $[Cl^-]_p$, has most probably a negligible contribution to dendritic $[Cl^-]_i$ dynamics.

One major finding of this study is the observation that a moderate GABAergic stimulation can induce substantial $[Cl^-]_i$ transients. In accordance with other studies, we observed that the $GABA_A$ receptor-mediated $[Cl^-]_i$ transients were altered if $E_m$ was set to depolarized and/or hyperpolarized values under voltage-clamp conditions (Backus et al., 1998; Kuner and Augustine, 2000; Raimondo et al., 2012a). However, the muscimol-induced $[Cl^-]_i$ transients are definitely overestimated under voltage-clamp conditions, because $DF_{Cl}$ was artificially stabilized by preventing voltage changes. But in the present study, we also applied the repetitive muscimol pulses under current-clamp conditions, when GABAergic currents shifted $E_m$ towards $E_{GABA}$ and thus reduce $DF_{Cl}$. These experiments revealed that even under these more physiological conditions, substantial $[Cl^-]_i$ transients are induced by activation of $GABA_A$ receptors. In the absence of voltage-clamp conditions several factors prevent that $DF_{Cl}$ will fade. Most importantly, the GABAergic hyperpolarization does not reach $E_{Cl}$ due to the persisting $HCO_3^-$ efflux *via* activated $GABA_A$ receptors (Grover et al., 1993; Rivera et al., 2005; Wright et al., 2011). In addition, the input conductances will stabilize $E_m$ and thus limit the GABAergic depolarization (Lombardi et al., 2019).

The second major finding of the present study is the observation that a coincident co-application of glutamate enhanced the muscimol-induced $[Cl^-]_i$ transients. To our knowledge a direct effect of synchronous glutamatergic depolarizations on GABA-induced $[Cl^-]_i$ transients has not been shown before, although it has been reported that the simultaneous activation of tonic GABAergic currents and glutamatergic currents by long-lasting glutamate applications induces massive $[Cl^-]_i$ changes (Deeb et al., 2011). Although from theoretical consideration each depolarizing current will enhance $DF_{Cl}$ and thus the $Cl^-$ fluxes through $GABA_A$

receptors (Farrant and Kaila, 2007; Kaila et al., 2014a), the present results are the first report that even moderate levels of glutamatergic stimulation, which were almost comparable to physiologically relevant levels of glutamatergic synaptic activity, are sufficient to enhance GABAergic $[Cl^-]_i$ transients. *via* this mechanism, the $[Cl^-]_i$ may serve as a kind of coincidence detector for glutamatergic and GABAergic inputs. If GABAergic and glutamatergic synapses are simultaneously activated, the $GABA_A$ receptor-dependent $[Cl^-]_i$ increase is augmented and thus a putative attenuation of the inhibitory capacity of $GABA_A$ receptors would be stronger. This coincident glutamatergic stimulation is in line with other mechanisms that promote a depolarized $E_m$ during GABAergic stimuli, like $HCO_3^-$-currents or activity-dependent $[K^+]_e$ transients (Kaila et al., 1997; Rivera et al., 2005; Wright et al., 2011), one additional factor enhancing activity-dependent shifts in GABAergic functions during moderate and massive synaptic activation.

The reduced inhibitory capacity induced by this activity-dependent $[Cl^-]_i$ increase may be an important element of short term plasticity (Jedlicka and Backus, 2006; Wright et al., 2011). Such a temporally limited and stimulus-dependent reduction of inhibition can e.g., attenuate feedforward and/or lateral inhibition and contribute to the gating of relevant information. In addition, this kind of ionic plasticity can also balance the short-term depression of glutamate release at synapses with high release probability (Gil et al., 1999). Thereby the observed influence of glutamatergic activity on ionic plasticity may serve to maintain excitation/inhibition ratio. Finally, the elevated $[Cl^-]_i$ upon ionic plasticity will enable larger glutamatergic depolarizations under co-activation of GABA and glutamate synapses, which may also facilitate the induction of long-term potentiation (Grover and Yan, 1999; Meredith et al., 2003; Ferando et al., 2016).

While the strong or pathophysiological stimuli used in most other studies result in massive changes in the $[Cl^-]_i$ (Ballanyi and Grafe, 1985; Isomura et al., 2003; Raimondo et al., 2015), the moderate GABAergic stimulation in our approach results in smaller and faster $[Cl^-]_i$ transients. Recovery of $[Cl^-]_i$ upon massive glutamatergic stimulation was still incomplete after 3 min (Moore et al., 2018) and the recovery after optogenetic $[Cl^-]_i$ loading showed requires ∼30 s (Raimondo et al., 2012a). In contrast, the present study demonstrated that the $[Cl^-]_i$ transients evoked by moderate GABAergic stimulation recovers within ∼5 s. This observation is in accordance with previous studies that reported that the $[Cl^-]_i$ transients upon a slightly stronger stimulus under voltage-clamp conditions also recovered within 15 s (Kuner and Augustine, 2000). We assume, that the faster recovery in our experiments reflects smaller $[Cl^-]_i$ transients with a restricted spatial extent. Another important observation of our study in this respect is the fact that the $[Cl^-]_i$ recovery of the activity-dependent $[Cl^-]_i$ transients is impaired in the presence of the KCC2 inhibitor VU0463271. This result implies that KCC2-mediated transmembrane transport constitutes the major factor in $[Cl^-]_i$ recovery, while a diffusion towards the soma is negligible. Thereby the fast KCC2-dependent recovery of $[Cl^-]_i$

determines the temporal properties of ionic plasticity. From the time course and functional consequences of the activity-dependent $[Cl^-]_i$ transients after moderate GABAergic stimuli, it is reasonable to consider that they contribute to short-term plasticity in the adult GABAergic system (Jedlicka and Backus, 2006; Wright et al., 2011).

The inhibition induced by $GABA_A$ receptors is mediated *via* membrane hyperpolarization and membrane shunting (Farrant and Kaila, 2007), with the membrane hyperpolarization depending on $DF_{Cl}$, i.e., of the difference between $E_m$ and $E_{Cl}$. Therefore, the $[Cl^-]_i$ increase after the repetitive stimulus will reduce the membrane hyperpolarization and thereby decrease the inhibitory capacity of GABAergic responses. Accordingly, we observed that the GABAergic rheobase shift, as a measure for the inhibitory capacity, was significantly attenuated by repetitive GABAergic stimulation. However, in all experiments GABA remained inhibitory, reflecting the fact that the shunting effect ensures that even depolarizing GABAergic responses mediate inhibition, as long as $E_{GABA}$ is negative to the AP threshold (Kolbaev et al., 2011a). It has been recently described that $[Cl^-]_i$ interferes with the excitability not only by its influence on $E_{GABA}$, but that the $[Cl^-]_i$ directly affects the AP threshold (Sørensen et al., 2017). While these experiments indicate that the increased $[Cl^-]_i$ induced by the activation of $GABA_A$ receptors should lead to a more hyperpolarized AP threshold and thus enhance excitability (Sørensen et al., 2017), we observed a higher rheobase, i.e., a lower excitability, after repetitive GABAergic stimulation. Probably the small $[Cl^-]_i$ changes observed in our experiments are insufficient to affect AP threshold (Sørensen et al., 2017).

However, while this significantly larger $[Cl^-]_i$ transient upon coincident glutamate/GABA receptor activation should in principle lead to a larger reduction in the inhibitory capacity of $GABA_A$ receptors, our experiments failed to find a significant reduction in the GABAergic rheobase shift after this stimulation paradigm. We propose that two electrophysiological properties may underlie this observation. First, the increased $[Cl^-]_i$ upon the coincident activation transfers in a non-linear fashion to only a slightly smaller membrane hyperpolarization (according to the Goldman-Hodgin-Katz equation; Farrant and Kaila, 2007). And second, the inhibitory effect of GABA was mediated by hyperpolarizing and by shunting inhibition (Farrant and Nusser, 2005; Mortensen et al., 2012). Thus the smaller hyperpolarizing inhibition upon a $[Cl^-]_i$ increase was probably masked by the remaining shunting inhibition and may thus limit the effects of moderate $[Cl^-]_i$ changes on GABAergic inhibition.

One additionally relevant information from our experiment is the fact that KCC2 plays an essential role for fast recovery of $[Cl^-]_i$ transients and therefore is the major constituent that limits ionic plasticity. This observation suggests that the amount of inhibition under frequent GABAergic synaptic inputs as well as the short-term depression of GABAergic inhibition upon short bursts of GABAergic inputs is controlled by the activity of KCC2. Therefore it is reasonable to suggest that even small alterations in the capacity of KCC2-mediated $Cl^-$-extrusion can impact

information processing *via* prolonged and enhanced activity-dependent $[Cl^-]_i$ transients within the dendritic compartment without leading to overt systematic $[Cl^-]_i$ changes, as has been demonstrated *in silico* (Doyon et al., 2016). Such less-controlled activity-dependent $[Cl^-]_i$ changes may also underlie the generation of seizure-like activity in patients with KCC2 mutations (Kahle et al., 2014b; Puskarjov et al., 2014b).

## DATA AVAILABILITY STATEMENT

The datasets generated for this study are available on request to the corresponding author.

## ETHICS STATEMENT

The animal study was reviewed and approved by Landesuntersuchungsanstalt RLP, Koblenz, Germany.

## AUTHOR CONTRIBUTIONS

WK and HL designed this study. LH performed the patch-clamp recordings. CA and AS performed the MEA recordings and the rtPCR experiments. LH, AS and WK analyzed the data. LH, AS, HL and WK wrote the manuscript.

## REFERENCES

Achilles, K., Okabe, A., Ikeda, M., Shimizu-Okabe, C., Yamada, J., Fukuda, A., et al. (2007). Kinetic properties of Cl uptake mediated by Na+-dependent $K^+$-2Cl cotransport in immature rat neocortical neurons. *J. Neurosci.* 27, 8616–8627. doi: 10.1523/jneurosci.5041-06.2007

Backus, K. H., Deitmer, J. W., and Friauf, E. (1998). Glycine-activated currents are changed by coincident membrane depolarization in developing rat auditory brainstem neurones. *J. Physiol.* 507, 783–794. doi: 10.1111/j.1469-7793.1998.783bs.x

Ballanyi, K., and Grafe, P. (1985). An intracellular analysis of gamma-aminobutyric-acid-associated ion movements in rat sympathetic neurones. *J. Physiol.* 365, 41–58. doi: 10.1113/jphysiol.1985.sp015758

Ben-Ari, Y. (2002). Excitatory actions of GABA during development: the nature of the nurture. *Nat. Rev. Neurosci.* 3, 728–739. doi: 10.1038/nrn920

Ben-Ari, Y., Woodin, M. A., Sernagor, E., Cancedda, L., Vinay, L., Rivera, C., et al. (2012). Refuting the challenges of the developmental shift of polarity of GABA actions: GABA more exciting than ever!. *Front. Cell. Neurosci.* 6:35. doi: 10.3389/fncel.2012.00035

Blaesse, P., Airaksinen, M. S., Rivera, C., and Kaila, K. (2009). Cation-chloride cotransporters and neuronal function. *Neuron* 61, 820–838. doi: 10.1016/j.neuron.2009.03.003

Blaesse, P., Guillemin, I., Schindler, J., Schweizer, M., Delpire, E., Khiroug, L., et al. (2006). Oligomerization of KCC2 correlates with development of inhibitory neurotransmission. *J. Neurosci.* 26, 10407–10419. doi: 10.1523/jneurosci.3257-06.2006

Cherubini, E., Gaiarsa, J. L., and Ben-Ari, Y. (1991). GABA: an excitatory transmitter in early postnatal life. *Trends Neurosci.* 14, 515–519. doi: 10.1016/0166-2236(91)90003-d

Deeb, T. Z., Lee, H. H. C., Walker, J. A., Davies, P. A., and Moss, S. J. (2011). Hyperpolarizing GABAergic transmission depends on KCC2 function and membrane potential. *Channels* 5, 475–481. doi: 10.4161/chan.5.6.17952

Doyon, N., Prescott, S. A., Castonguay, A., Godin, A. G., Kroger, H., and De Koninck, Y. (2011). Efficacy of synaptic inhibition depends on multiple, dynamically interacting mechanisms implicated in chloride homeostasis. *PLoS Comput. Biol.* 7:e1002149. doi: 10.1371/journal.pcbi.1002149

Doyon, N., Prescott, S. A., and De Koninck, Y. (2016). Mild KCC2 hypofunction causes inconspicuous chloride dysregulation that degrades neural coding. *Front. Cell. Neurosci.* 9:516. doi: 10.3389/fncel.2015.00516

Ebihara, S., Shirato, K., Harata, N., and Akaike, N. (1995). Gramicidin-perforated patch recording: GABA response in mammalian neurones with intact intracellular chloride. *J. Physiol.* 484, 77–86. doi: 10.1113/jphysiol.1995.sp020649

Fagiolini, M., Fritschy, J. M., Löw, K., Möhler, H., Rudolph, U., and Hensch, T. K. (2004). Specific $GABA_A$ circuits for visual cortical plasticity. *Science* 303, 1681–1683. doi: 10.1126/science.1091032

Farrant, M., and Kaila, K. (2007). The cellular, molecular and ionic basis of $GABA_A$ receptor signalling. *Prog. Brain Res.* 160, 59–87. doi: 10.1016/S0079-6123(06)60005-8

Farrant, M., and Nusser, Z. (2005). Variations on an inhibitory theme: phasic and tonic activation of $GABA_A$ receptors. *Nat. Rev. Neurosci.* 6, 215–229. doi: 10.1038/nrn1625

Ferando, I., Faas, G. C., and Mody, I. (2016). Diminished KCC2 confounds synapse specificity of LTP during senescence. *Nat. Neurosci.* 19, 1197–1200. doi: 10.1038/nn.4357

Fujiwara-Tsukamoto, Y., Isomura, Y., Nambu, A., and Takada, M. (2003). Excitatory GABA input directly drives seizure-like rhythmic synchronization in mature hippocampal CA1 pyramidal cells. *Neuroscience* 119, 265–275. doi: 10.1016/s0306-4522(03)00102-7

Gagnon, M., Bergeron, M. J., Lavertu, G., Castonguay, A., Tripathy, S., Bonin, R. P., et al. (2013). Chloride extrusion enhancers as novel therapeutics for neurological diseases. *Nat. Med.* 19, 1524–1528. doi: 10.1038/nm.3356

Ganguly, K., Schinder, A. F., Wong, S. T., and Poo, M. (2001). GABA itself promotes the developmental switch of neuronal GABAergic responses from excitation to inhibition. *Cell* 105, 521–532. doi: 10.1016/s0092-8674(01)00341-5

Gil, Z., Connors, B. W., and Amitai, Y. (1999). Efficacy of thalamocortical and intracortical synaptic connections: quanta, innervation, and reliability. *Neuron* 23, 385–397. doi: 10.1016/s0896-6273(00)80788-6

Grover, L. M., Lambert, N. A., Schwartzkroin, P. A., and Teyler, T. J. (1993). Role of HCO3- ion in depolarizing $GABA_A$ receptor mediated responses in pyramidal cells in hippocampus. *J. Neurophysiol.* 69, 1541–1555. doi: 10.1152/jn.1993.69.5.1541

Grover, L. M., and Yan, C. (1999). Blockade of $GABA_A$ receptors facilitates induction of NMDA receptor-independent long-term potentiation. *J. Neurophysiol.* 81, 2814–2822. doi: 10.1152/jn.1999.81.6.2814

Isomura, Y., Sugimoto, M., Fujiwara-Tsukamoto, Y., Yamamoto-Muraki, S., Yamada, J., and Fukuda, A. (2003). Synaptically activated $Cl^-$ accumulation responsible for depolarizing GABAergic responses in mature hippocampal neurons. *J. Neurophysiol.* 90, 2752–2756. doi: 10.1152/jn.00142.2003

Jarolimek, W., Lewen, A., and Misgeld, U. (1999). A furosemide-sensitive $K^+$-$Cl^-$ cotransporter counteracts intracellular $Cl^-$ accumulation and

depletion in cultured rat midbrain neurons. *J. Neurosci.* 19, 4695–4704. doi: 10.1523/jneurosci.19-12-04695.1999

Jedlicka, P., and Backus, K. H. (2006). Inhibitory transmission, activity-dependent ionic changes and neuronal network oscillations. *Physiol. Res.* 55, 139–149.

Jedlicka, P., Deller, T., Gutkin, B. S., and Backus, K. H. (2011). Activity-dependent intracellular chloride accumulation and diffusion controls GABA$_A$ receptor-mediated synaptic transmission. *Hippocampus* 21, 885–898. doi: 10.1002/hipo.20804

Jonas, P., Bischofberger, J., Fricker, D., and Miles, R. (2004). Interneuron diversity series: fast in, fast out--temporal and spatial signal processing in hippocampal interneurons. *Trends Neurosci.* 27, 30–40. doi: 10.1016/j.tins.2003.10.010

Kahle, K. T., Khanna, A., Clapham, D. E., and Woolf, C. J. (2014a). Therapeutic restoration of spinal inhibition *via* druggable enhancement of potassium-chloride cotransporter KCC2-mediated chloride extrusion in peripheral neuropathic pain. *JAMA Neurol.* 71, 640–645. doi: 10.1001/jamaneurol.2014.21

Kahle, K. T., Merner, N. D., Friedel, P., Silayeva, L., Liang, B., Khanna, A., et al. (2014b). Genetically encoded impairment of neuronal KCC2 cotransporter function in human idiopathic generalized epilepsy. *EMBO Rep.* 15, 766–774. doi: 10.15252/embr.201438840

Kahle, K. T., Staley, K. J., Nahed, B. V., Gamba, G., Hebert, S. C., Lifton, R. P., et al. (2008). Roles of the cation-chloride cotransporters in neurological disease. *Nat. Clin. Pract. Neurol.* 4, 490–503. doi: 10.1038/ncpneuro0883

Kaila, K., Lamsa, K., Smirnov, S., Taira, T., and Viopio, J. (1997). Long-lasting GABA-mediated depolarization evoked by high-frequency stimulation in pyramidal neurons of rat hippocampal slice is attributable to a network-driven, bicarbonate-dependent K$^+$ transient. *J. Neurosci.* 17, 7662–7672. doi: 10.1523/jneurosci.17-20-07662.1997

Kaila, K., Price, T. J., Payne, J. A., Puskarjov, M., and Voipio, J. (2014a). Cation-chloride cotransporters in neuronal development, plasticity and disease. *Nat. Rev. Neurosci.* 15, 637–654. doi: 10.1038/nrn3819

Kaila, K., Ruusuvuori, E., Seja, P., Voipio, J., and Puskarjov, M. (2014b). GABA actions and ionic plasticity in epilepsy. *Curr. Opin. Neurobiol.* 26, 34–41. doi: 10.1016/j.conb.2013.11.004

Kilb, W., Kirischuk, S., and Luhmann, H. J. (2013). Role of tonic GABAergic currents during pre- and early postnatal rodent development. *Front. Neural Circuits* 7:139. doi: 10.3389/fncir.2013.00139

Kolbaev, S. N., Achilles, K., Luhmann, H. J., and Kilb, W. (2011a). Effect of depolarizing GABA$_A$-mediated membrane responses on excitability of Cajal-Retzius cells in the immature rat neocortex. *J. Neurophysiol.* 106, 2034–2044. doi: 10.1152/jn.00699.2010

Kolbaev, S. N., Luhmann, H. J., and Kilb, W. (2011b). Activity-dependent scaling of GABAergic excitation by dynamic Cl$^-$ changes in Cajal-Retzius cells. *Pflugers Arch.* 461, 557–565. doi: 10.1007/s00424-011-0935-4

Kuner, T., and Augustine, G. J. (2000). A genetically encoded ratiometric indicator for chloride: capturing chloride transients in cultured hippocampal neurons. *Neuron* 27, 447–459. doi: 10.1016/s0896-6273(00)00056-8

Kyrozis, A., and Reichling, D. B. (1995). Perforated-patch recording with gramicidin avoids artifactual changes in intracellular chloride concentration. *J. Neurosci. Methods* 57, 27–35. doi: 10.1016/0165-0270(94)00116-x

Lavertu, G., Côté, S. L., and De Koninck, Y. (2014). Enhancing K-Cl co-transport restores normal spinothalamic sensory coding in a neuropathic pain model. *Brain* 137, 724–738. doi: 10.1093/brain/awt334

Lombardi, A., Jedlicka, P., Luhmann, H. J., and Kilb, W. (2018). Giant depolarizing potentials trigger transient changes in the intracellular Cl$^-$ concentration in CA3 pyramidal neurons of the immature mouse hippocampus. *Front. Cell. Neurosci.* 12:420. doi: 10.3389/fncel.2018.00420

Lombardi, A., Jedlicka, P., Luhmann, J. H., and Kilb, W. (2019). Interactions between membrane resistance, GABA-A receptor properties, bicarbonate dynamics and Cl$^-$-transport shape activity-dependent changes of intracellular Cl$^-$ concentration. *Int. J. Mol. Sci.* 20:E1416. doi: 10.3390/ijms20061416

Löscher, W., Puskarjov, M., and Kaila, K. (2013). Cation-chloride cotransporters NKCC1 and KCC2 as potential targets for novel antiepileptic and antiepileptogenic treatments. *Neuropharmacology* 69, 62–74. doi: 10.1016/j.neuropharm.2012.05.045

Meredith, R. M., Floyer-Lea, A. M., and Paulsen, O. (2003). Maturation of long-term potentiation induction rules in rodent hippocampus: role of GABAergic inhibition. *J. Neurosci.* 23, 11142–11146. doi: 10.1523/jneurosci.23-35-11142.2003

Mody, I., and Pearce, R. A. (2004). Diversity of inhibitory neurotransmission through GABA$_A$ receptors. *Trends Neurosci.* 27, 569–575. doi: 10.1016/j.tins.2004.07.002

Mohapatra, N., Tønnesen, J., Vlachos, A., Kuner, T., Deller, T., Nagerl, U. V., et al. (2016). Spines slow down dendritic chloride diffusion and affect short-term ionic plasticity of GABAergic inhibition. *Sci. Rep.* 6:23196. doi: 10.1038/srep23196

Moore, Y. E., Deeb, T. Z., Chadchankar, H., Brandon, N. J., and Moss, S. J. (2018). Potentiating KCC2 activity is sufficient to limit the onset and severity of seizures. *Proc. Natl. Acad. Sci. U S A* 115, 10166–10171. doi: 10.1073/pnas.1810134115

Mortensen, M., Patel, B., and Smart, T. G. (2012). GABA potency at GABA$_A$ receptors found in synaptic and extrasynaptic zones. *Front. Cell. Neurosci.* 6:1. doi: 10.3389/fncel.2012.00001

Pfaffl, M. W., Horgan, G. W., and Dempfle, L. (2002). Relative expression software tool (REST©) for group-wise comparison and statistical analysis of relative expression results in real-time PCR. *Nucleic Acids Res.* 30:e36. doi: 10.1093/nar/30.9.e36

Pouille, F., and Scanziani, M. (2004). Routing of spike series by dynamic circuits in the hippocampus. *Nature* 429, 717–723. doi: 10.1038/nature02615

Pusch, M., and Neher, E. (1988). Rates of diffusional exchange between small cells and a measuring patch pipette. *Pflugers Arch.* 411, 204–211. doi: 10.1007/bf00582316

Puskarjov, M., Kahle, K. T., Ruusuvuori, E., and Kaila, K. (2014a). Pharmacotherapeutic targeting of cation-chloride cotransporters in neonatal seizures. *Epilepsia* 55, 806–818. doi: 10.1111/epi.12620

Puskarjov, M., Seja, P., Heron, S. E., Williams, T. C., Ahmad, F., Iona, X., et al. (2014b). A variant of KCC2 from patients with febrile seizures impairs neuronal Cl$^-$ extrusion and dendritic spine formation. *EMBO Rep.* 15, 723–729. doi: 10.1002/embr.201438749

Raimondo, J. V., Burman, R. J., Katz, A. A., and Akerman, C. J. (2015). Ion dynamics during seizures. *Front. Cell. Neurosci.* 9:419. doi: 10.3389/fncel.2015.00419

Raimondo, J. V., Kay, L., Ellender, T. J., and Akerman, C. J. (2012a). Optogenetic silencing strategies differ in their effects on inhibitory synaptic transmission. *Nat. Neurosci.* 15, 1102–1104. doi: 10.1038/nn.3143

Raimondo, J. V., Markram, H., and Akerman, C. J. (2012b). Short-term ionic plasticity at GABAergic synapses. *Front. Synaptic Neurosci.* 4:5. doi: 10.3389/fnsyn.2012.00005

Rivera, C., Voipio, J., and Kaila, K. (2005). Two developmental switches in GABAergic signalling: the K$^+$-Cl$^-$ cotransporter KCC2 and carbonic anhydrase CAVII. *J. Physiol.* 562, 27–36. doi: 10.1113/jphysiol.2004.077495

Rivera, C., Voipio, J., Payne, J. A., Ruusuvuori, E., Lahtinen, H., Lamsa, K., et al. (1999). The K$^+$/Cl$^-$ co-transporter KCC2 renders GABA hyperpolarizing during neuronal maturation. *Nature* 397, 251–255. doi: 10.1038/16697

Silayeva, L., Deeb, T. Z., Hines, R. M., Kelley, M. R., Munoz, M. B., Lee, H. H. C., et al. (2015). KCC2 activity is critical in limiting the onset and severity of status epilepticus. *Proc. Natl. Acad. Sci. U S A* 112, 3523–3528. doi: 10.1073/pnas.1415126112

Sivakumaran, S., Cardarelli, R. A., Maguire, J., Kelley, M. R., Silayeva, L., Morrow, D. H., et al. (2015). Selective inhibition of KCC2 leads to hyperexcitability and epileptiform discharges in hippocampal slices and *in vivo*. *J. Neurosci.* 35, 8291–8296. doi: 10.1523/jneurosci.5205-14.2015

Sørensen, A. T., Ledri, M., Melis, M., Nikitidou Ledri, L., Andersson, M., and Kokaia, M. (2017). Altered chloride homeostasis decreases the action potential threshold and increases hyperexcitability in hippocampal neurons. *eNeuro* 4:ENEURO.0172–17.2017. doi: 10.1523/eneuro.0172-17.2017

Staley, K. J., Soldo, B. L., and Proctor, W. R. (1995). Ionic mechanisms of neuronal excitation by inhibitory GABA$_A$ receptors. *Science* 269, 977–981. doi: 10.1126/science.7638623

Sun, J. J., Kilb, W., and Luhmann, H. J. (2010). Self-organization of repetitive spike patterns in developing neuronal networks *in vitro*. *Eur. J. Neurosci.* 32, 1289–1299. doi: 10.1111/j.1460-9568.2010.07383.x

Thompson, S. M., and Gähwiler, B. H. (1989). Activity-dependent disinhibition. I. Repetitive stimulation reduces IPSP driving force and conductance in the hippocampus *in vitro*. *J. Neurophysiol.* 61, 501–511. doi: 10.1152/jn.1989.61.3.501

Titz, S., Hans, M., Kelsch, W., Lewen, A., Swandulla, D., and Misgeld, U. (2003). Hyperpolarizing inhibition develops without trophic support by GABA in cultured rat midbrain neurons. *J. Physiol.* 550, 719–730. doi: 10.1113/jphysiol.2003.041863

Wagenaar, D. A., Pine, J., and Potter, S. M. (2006). An extremely rich repertoire of bursting patterns during the development of cortical cultures. *BMC Neurosci.* 7:11. doi: 10.1186/1471-2202-7-11

Weir, K., Blanquie, O., Kilb, W., Luhmann, H. J., and Sinning, A. (2015). Comparison of spike parameters from optically identified GABAergic and glutamatergic neurons in sparse cortical cultures. *Front. Cell. Neurosci.* 8:460. doi: 10.3389/fncel.2014.00460

Whittington, M. A., and Traub, R. D. (2003). Interneuron diversity series: inhibitory interneurons and network oscillations *in vitro*. *Trends Neurosci.* 26, 676–682. doi: 10.1016/j.tins.2003.09.016

Wright, R., Raimondo, J. V., and Akerman, C. J. (2011). Spatial and temporal dynamics in the ionic driving force for $GABA_A$ receptors. *Neural Plast.* 2011:728395. doi: 10.1155/2011/728395

**Conflict of Interest**: The authors declare that the research was conducted in the absence of any commercial or financial relationships that could be construed as a potential conflict of interest.